Human Molecular Genetics, 2015, 1–14

doi: 10.1093/hmg/ddv179
Advance Access Publication Date: 13 May 2015
Original Article

ORIGINAL ARTICLE

TBK1 controls autophagosomal engulfment of polyubiquitinated mitochondria through p62/SQSTM1 phosphorylation

Gen Matsumoto[1,3,4,5,†,*], Tomomi Shimogori[4], Nobutaka Hattori[2] and Nobuyuki Nukina[1,3,4,5,‡,*]

[1]Department of Neuroscience for Neurodegenerative Disorders and [2]Department of Neurology, Juntendo University Graduate School of Medicine, Bunkyo-ku, Tokyo 113-8421, Japan, [3]Laboratory for Structural Neuropathology and [4]Laboratory for Molecular Mechanisms of Thalamus Development, RIKEN Brain Science Institute, 2-1 Hirosawa, Wako, Saitama 351-0198, Japan and [5]Core Research for Evolutionary Science and Technology (CREST), JST, 7, Gobancho, Chiyoda-ku, Tokyo 102-0076, Japan

*To whom correspondence should be addressed at: Department of Neuroscience for Neurodegenerative Disorders, Juntendo University Graduate School of Medicine, 2-1-1 Hongo, Bunkyo-ku, Tokyo 113-8421, Japan. Tel: +81 356841370; Fax: +81 356841370; Email: nnukina@juntendo.co.jp (N.N.)/g-matsumoto@nagasaki-u.ac.jp (G.M.)

Abstract

Selective autophagy adaptor proteins, including p62/SQSTM1, play pivotal roles in the targeted degradation of ubiquitinated proteins or organelles through the autophagy-lysosome system. However, how autophagy adaptors promote the autophagosomal engulfment of selected substrates is poorly understood. Here, we show that p62 phosphorylation at S403 is required for the efficient autophagosomal engulfment of polyubiquitinated mitochondria during Parkin-dependent mitophagy. p62 is able to interact with Parkin-recruited mitochondria without S403 phosphorylation under mitophagy-inducing conditions, but those mitochondria are not enclosed by autophagosomes. Intriguingly, the S403 phosphorylation occurs only in the early period of mitochondrial depolarization. Optineurin and TANK-binding kinase 1 (TBK1) are transiently recruited to the polyubiquitinated mitochondria, and the activated TBK1 phosphorylates p62 at S403. TBK1 inhibitor, BX795, prevents the p62-mediated autophagosomal engulfment of Parkin-recruited mitochondria. Our results suggest that TBK1-mediated S403 phosphorylation regulates the efficient autophagosomal engulfment of ubiquitinated mitochondria as an immediate response to the mitochondrial depolarization.

Introduction

Selective clearance of misfolded proteins, damaged organelles or invading pathogens through macroautophagy (autophagy) is a critical program for cellular protection. Canonical autophagy has been established as a process for bulk (random) protein degradation in which autophagosomes contain cytoplasmic proteins and organelles without any substrate specificity, whereas selective autophagy refers to the selective engulfment of autophagic cargo by autophagosomes (1,2). Substrate selectivity is provided to autophagosomes by autophagic adaptor proteins (also known as autophagy receptors) that contain an LC3-interacting region and polyubiquitin-binding motifs to connect ubiquitinated autophagic substrates to autophagosomes (2,3).

[†]Present address: Department of Anatomy and Neurobiology, Nagasaki University School of Medicine, 1-12-4 Sakamoto, Nagasaki 852-8523, Japan.
[‡]Present address: Laboratory of Structural Neuropathology, Doshisha University Graduate School of Brain Science, Kyoto 610-0394, Japan.
Received: January 31, 2015. **Revised:** April 28, 2015. **Accepted:** May 11, 2015

p62/SQSTM1 is the best characterized autophagic adaptor protein and participates in various kinds of selective autophagy (2,4,5). We have previously demonstrated that p62 is multiply phosphorylated and a phosphorylation at serine 403 (S403) enhances its autophagic degradation (6). The S403 locates at the interface between ubiquitin and p62 ubiquitin-associated (UBA) domain, and the phospho-S403 is predicted to form important polar contacts with the side chains of Lys 6 and His 68 on ubiquitin (7). The S403 phosphorylation alters the affinity between p62 and polyubiquitin chain, allowing efficient targeting of polyubiquitinated proteins to autophagosomes. The S403-phosphorylated p62 is continuously degraded through constitutive autophagy together with ubiquitinated substrates (6). Because purified p62 has only a weak affinity against K63-linked polyubiquitin chains and almost no binding property to K48-linked polyubiquitin chains *in vitro* (6,8), proteasomal substrates, which have K48-linked polyubiquitin chains, cannot be a substrate of p62-mediated selective autophagy without S403 phosphorylation. Whereas the S403-phosphorylated p62 binds to both types of polyubiquitin chains with higher affinity, thus S403-phospho-p62-mediated selective autophagy plays an essential role in a compensatory mechanism for the ubiquitin–proteasome system (UPS) (6,9,10). However, it remains unclear whether the S403-phosphorylated p62 enhances also the selective autophagosomal engulfment of cellular components.

The S403 phosphorylation of p62 is catalyzed by casein kinase 2 (CK2) (6) and TANK-binding kinase 1 (TBK1) (11). CK2 is a versatile, constitutively active kinase (12), whereas TBK1 is a master regulator of the type I interferon response in the cellular pathogen defense system. This defense system is stringently downregulated under normal conditions (13), but upon bacterial invasion, the cell attempts to eliminate the bacteria through xenophagy. The innate cellular immune system activates TBK1, which directly catalyzes p62 phosphorylation at S403 during xenophagy (11), but it is not known whether TBK1-mediated signaling participates in other selective autophagy processes without pathogen invasion.

Mitochondrial dysfunction has been implicated as a key pathway for neuronal degeneration in many age-related neurodegenerative disorders (14,15), because damaged mitochondria are a major source of reactive oxygen species (ROS) (16). Parkin-dependent mitophagy is one of the best-characterized pathways for the degradation of depolarized mitochondria (17,18). Parkin is a cytoplasmic E3 ubiquitin ligase and marks depolarized mitochondria by attaching K63-linked polyubiquitin chain to numerous target molecules in the outer mitochondrial membrane (19–21). The Parkin-ubiquitinated mitochondria are subjected to degradation through both autophagy and UPS (22,23). Since autophagosomes including mitochondria are observed during mitochondrial depolarization by electron microscopy, it is clear that the damaged mitochondria are removed by autophagy. However, how autophagosomes enclose the ubiquitin-tagged mitochondria and how autophagic adaptor proteins elicit the mitophagy still remain unclear.

In this report, we show that p62 phosphorylation at S403 is required for the promotion of autophagosomal engulfment of ubiquitinated mitochondria and this p62 phosphorylation depends on the activated TBK1. During Parkin-dependent mitophagy, p62 accumulates at Parkin-recruited mitochondria, but only the S403-phosphorylated p62-containing mitochondria are enclosed by autophagosomes. The mitophagy-induced S403 phosphorylation occurs only in the early time period of mitochondrial depolarization. TBK1 kinase inhibitor prevents the p62 phosphorylation and reduces autophagosomal engulfment. Although TBK1 is inactivated under normal conditions, optineurin (OPTN)-mediated TBK1 mitochondrial relocation induces TBK1 activation and S403 phosphorylation of p62 at Parkin-recruited mitochondria. Our results suggest that TBK1-mediated p62 phosphorylation regulates the efficient autophagosomal engulfment of mitochondria as an acute response and that OPTN–TBK1-p62 co-localization at ubiquitin-tagged cargo may be a common determinant for the autophagosomal engulfment in different types of selective autophagy.

Results

p62 is S403 phosphorylated during mitochondrial depolarization

We previously demonstrated that a phosphorylation at S403 of p62 has important roles in the selective autophagic degradation of ubiquitinated proteins, (6) and Pilli *et al.* also revealed that the phosphorylation occurs in autophagic elimination of invading bacteria, xenophagy (11). To investigate whether the S403 phosphorylation has a role in mitophagy, we first explored the phosphorylation and degradation of p62 during Parkin-dependent mitophagy in neuronal cells. As cultured mouse neuroblastoma Neuro2a cells (N2a) did not express a detectable level of endogenous Parkin protein (data not shown), we developed an N2a-derived cell line stably expressing RFP-Parkin (R-Parkin). Consistent with previous studies (24–26), R-Parkin formed punctate structures (describe as Parkin puncta here after) upon a treatment with carbonyl cyanide *m*-chlorophenyl hydrazine (CCCP), a mitochondrial uncoupler, for 3 h and clustered in 6 h of treatment. In the early time period of CCCP treatment, up to 3 h, >90% of R-Parkin puncta contained both p62 and Tom20, a mitochondrial outer membrane protein (Supplementary Material, Fig. S1C), although the large fraction of mitochondria was without R-Parkin or p62 (Fig. 1A and Supplementary Material, Fig. S1A–D). The Parkin puncta grew larger involving mitochondria during the CCCP treatment and formed large-sized mitochondria cluster. Because p62 did not co-localize with normal or depolarized mitochondria without Parkin, Parkin was required for the p62 recruitment to mitochondria (Supplementary Material, Fig. S1A and B). Polyubiquitin was also detected in the Parkin-positive mitochondria, but not in Parkin-free mitochondria, confirming that Parkin-recruited mitochondria were polyubiquitinated (Fig. 1A bottom). These results demonstrate that Parkin puncta represents the Parkin-recruited polyubiquitinated mitochondria, and the depolarized mitochondria are an appropriate substrate for p62-mediated selective autophagy in neuronal cells.

p62 S403 phosphorylation occurs transiently even in the continuous mitochondrial depolarization condition

In the early time period of CCCP treatment, for 3 h, S403-phosphorylated p62 is detected in the Parkin puncta that represented polyubiquitinated mitochondria (Fig. 1A middle and B). Unexpectedly, we observed that several R-Parkin puncta with p62 were not S403 phosphorylated (Fig. 1B arrowheads), even though nearly all R-Parkin puncta were co-localized with p62 (Fig. 1B and Supplementary Material, Fig. S1C). The presence or absence of S403-phosphorylated p62 in a Parkin punctum was not due to fluorophore propensity, because both GFP- and RFP-Parkin-expressing N2a cell lines showed the same results (Fig. 1B and Supplementary Material, Fig. S2B). These results indicate that Parkin-recruited mitochondria are grouped into two distinct

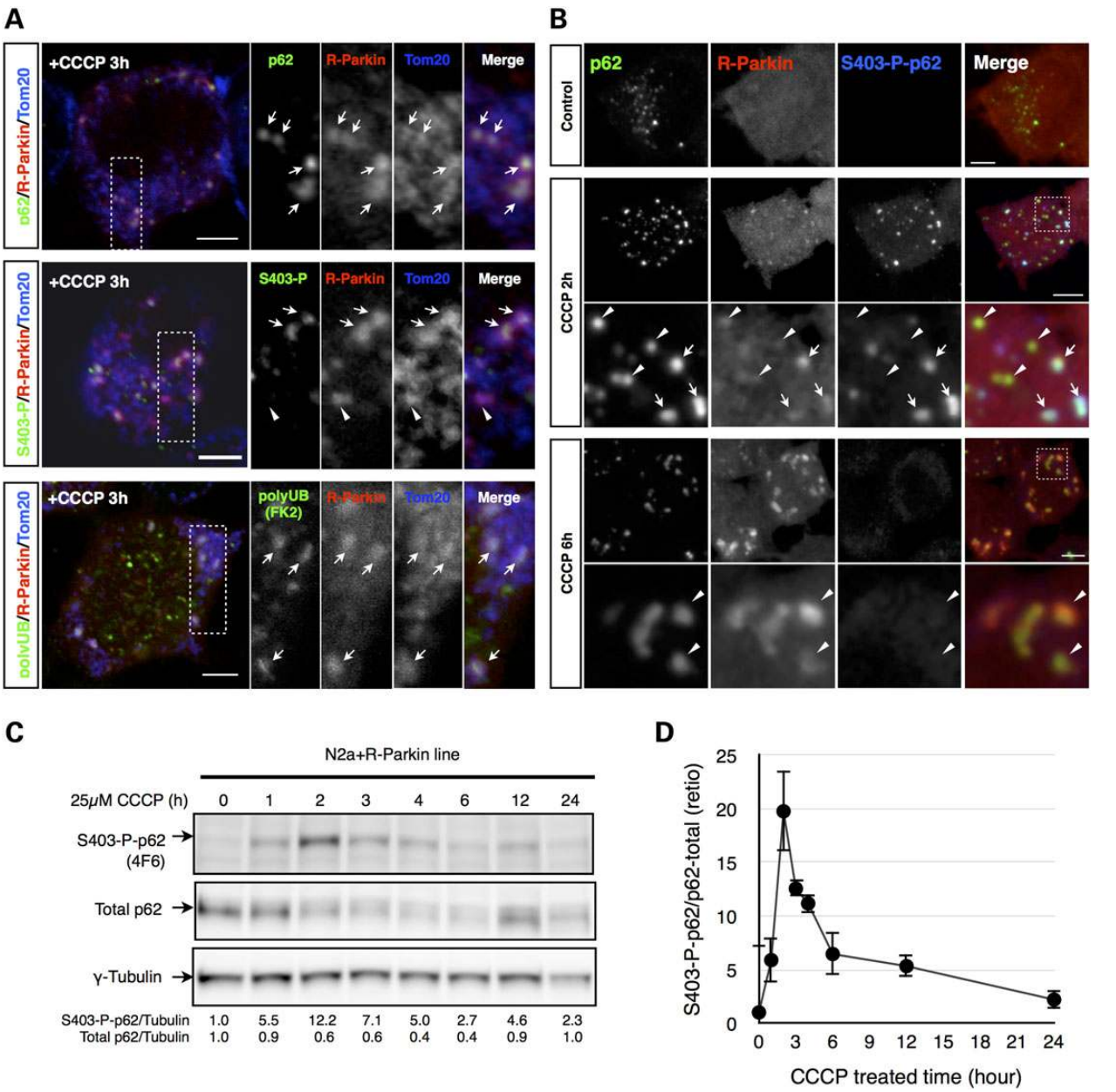

Figure 1. p62 is transiently phosphorylated at S403 during mitochondrial depolarization. (**A**) N2a cells stably expressing R-Parkin were treated with 25 μM CCCP for 3 h, and total endogenous p62 (p62; top, green), S403-phospho-p62 (S403-P; middle, green), polyubiquitin (polyUb(FK2); bottom, green), R-Parkin (red) and Tom20 (blue) were visualized by confocal microscopy as indicated. Magnified images corresponding to rectangle region in merged images were generated in each fluorophore as indicated. Arrows and arrowheads indicate the Tom20-positive Parkin puncta and the S403-phospho-p62-negative Parkin puncta, respectively. Scale bar = 5 μm. (**B**) Cells in A were treated with 25 μM CCCP for the indicated periods, and total endogenous p62 (p62; green), R-Parkin (red) and S403-phospho-p62 (S403-P; blue) were visualized by confocal microscopy as indicated. Magnified images corresponding to rectangle region in merged images are shown. Arrows and arrowheads indicate the S403-phospho-p62-positive and the S403-phospho-p62-negative Parkin puncta, respectively. Scale bar = 5 μm. (**C**) Cells in A were treated with 25 μM CCCP for indicated periods. S403 phosphorylation level and total amount of p62 were analyzed by western blotting. The γ-tubulin normalized relative amounts of S403-phospho-p62, and total p62 are shown. (**D**) The S403 phosphorylation ratio of p62 described in B is shown. Error bar represents standard error of the mean (SEM) ($n = 4$).

classes, such as those with or without S403-phospho-p62 in a punctum, and that p62 is able to interact with Parkin-recruited mitochondria without S403 phosphorylation.

After 6 hours of CCCP treatment, Parkin-recruited mitochondria formed mitochondria clusters, but S403-phosphorylated p62 was not observed in them. (Fig. 1B and Supplementary Material, Fig. S1B). Immunoblotting analysis revealed that the S403-phosphorylated p62 appeared only in the early time period of CCCP treatment and the S403-phospho-p62 disappeared after that, even though the mitochondrial depolarization was continued (Fig. 1C and D). The disappearance of S403-phosphorylated p62 was due to the autophagic degradation, because Bafilomycin A1 (BafA) treatment, which blocked autophagosome-lysosome fusion, protected the S403-phospho-p62 (Supplementary Material, Fig. S2A).

We next determined whether S403 phosphorylation of p62 depended on Parkin-mediated polyubiquitination. As consistent with previous reports (25,26), Parkin mutants (K161N and G430D),

which were deficient in ubiquitin E3 ligase activity, did not show any Parkin puncta and co-localization with Parkin and p62 (Supplementary Material, Fig. S3A). The p62 degradation, S403 phosphorylation and Parkin self-polyubiquitination were not observed under the CCCP-treated conditions, suggesting that p62-mediated mitophagy did not occur without Parkin's E3 ligase activity (Supplementary Material, Fig. S3B). The D280N mutant that retained E3 ligase activity formed p62-positive Parkin puncta and induced S403 phosphorylation as well as wild type, supporting that Parkin E3 ubiquitin ligase activity is essential for the induction of p62 phosphorylation (Supplementary Material, Fig. S3A and B).

p62 S403 Phosphorylation is required for the efficient autophagosomal engulfment

To investigate the consequence of the S403 phosphorylation in Parkin puncta, we analyzed the distribution of S403-phosphorylated p62 in autophagosomes by monitoring GFP-LC3 (G-LC3), R-Parkin and S403-phospho-p62. We found that Parkin puncta co-localizing with G-LC3 were S403 phosphorylation positive, even though many autophagosomes (or LC3-positive phagophores) were observed throughout the cell (Fig. 2A). The Parkin puncta including the mitochondrial matrix chaperone Hsp60 were surrounded by G-LC3-positive autophagosomes (Fig. 2B), and the Parkin puncta co-localizing with Lamp2A, a lysosomal protein, were also detected (Fig. 2C), confirming that this autophagosomal engulfment of the Parkin punctum is in a process of mitophagy. The number of autophagosomes was reduced in accordance with the attenuation of p62 phosphorylation, and G-LC3 signals were excluded from mitochondria clusters after 6 h of treatment with CCCP (Fig. 2A bottom). These results suggest that autophagosomes require the p62 S403 phosphorylation to engulf the Parkin-recruited mitochondria efficiently in the early phase of mitophagy. It may be worth to note that the degradation of mitochondria is hardly detected by the reduction of mitochondrial protein in the early time point of CCCP treatment, as the most of depolarized mitochondria remain without Parkin at that time (Fig. 1A and Supplementary Material, Fig. S1A).

TBK1 phosphorylates p62 during Parkin-dependent mitophagy

The existence of two distinct types of Parkin puncta indicates that p62 is phosphorylated within a Parkin punctum, and the responsible kinase may be activated after the Parkin punctum formation. Since CK2 and TBK1 have been identified in S403 phosphorylation, we first tested whether these kinase inhibitors prevent the S403 phosphorylation during Parkin-dependent mitophagy. A TBK1 inhibitor, BX795, clearly prevented CCCP-induced S403 phosphorylation, but a CK2 inhibitor, 4,5,6,7-tetrabromobenzotriazole, did not (Supplementary Material, Fig. S4A), indicating that TBK1 participated in this process. To determine whether the TBK1 is activated by CCCP treatment, we monitored S172 phosphorylation of TBK1, which is essential for TBK1 activation (27). Under normal conditions, S172-phosphorylated TBK1 was not detected in cells, confirming its inactivation (Fig. 3A, top panels). S172-phospho-TBK1 appeared after CCCP treatment and also was co-localized with S403-phospho-p62 in Parkin puncta (Fig. 3A, second panels). Increased numbers of Parkin puncta containing both S172-phospho-TBK1 and S403-phospho-p62 were observed in cells treated with both CCCP and BafA. BX795 treatment prevented both TBK1 and p62 phosphorylation during mitophagy (Fig. 3A, third and bottom panels). As well as S403-phospho-p62, the S172-phospho-TBK1 was also detected in G-LC3 positive-autophagosomes after 3 hours of CCCP treatment, but not after 6 h (Fig. 3B), suggesting that the attenuation of p62 S403 phosphorylation might be caused by the absence of active TBK1.

If S403-phosphorylated p62 has a critical role in the autophagosomal engulfment, Parkin puncta without S403-phospho-p62 should be excluded from autophagosomes. To test this, we analyzed the G-LC3-present or G-LC3-absent Parkin puncta under TBK1-activated or TBK1-inhibited conditions (Fig. 4A–C). Because autophagosomes were rapidly degraded during CCCP treatment, we protect autophagosomes from their lysosomal degradation by BafA treatment and counted the total number of R-Parkin-positive autophagosomes with or without G-LC3 in whole-cell images. About 70% of Parkin puncta were co-localized with both G-LC3 and S403-phospho-p62 under CCCP- and BafA-treated conditions (Fig. 4A and B). In contrast, the number of Parkin puncta surrounded by G-LC3 was obviously decreased by the BX795 treatment (21.5%). As autophagosome accumulation was observed when cells are treated with both CCCP and BX795, BX795 treatment itself did not affect the autophagosome formation (Fig. 4A). Western blot analysis showed that BX795 treatment significantly repressed the CCCP-induced p62 degradation as well as S403 phosphorylation (Fig. 4C and D). These results support the idea that TBK1 signaling regulates the autophagosomal engulfment of mitochondria through S403 phosphorylation of p62.

We next investigate how TBK1 is activated during Parkin-mediated mitophagy. It has been proposed that TBK1 activation is primarily regulated by local concentration through the trans-autophosphorylation mechanism (28,29). If the TBK1 is locally concentrated at Parkin puncta and activated though this mechanism, the kinase dead mutant TBK1 (K38M) (30) may work as dominant negative. Consistent with previous results (31), the overexpressed wild-type R-TBK1 was constitutively S172 phosphorylated (Fig. 4E). Although the overexpressed wild-type R-TBK1 is active, the S403 phosphorylation of p62 was not enhanced under normal conditions. By the CCCP treatment, the amount of S172-phosphorylated TBK1 and that of S403-phosphorylated p62 were obviously increased. The S172-phosphorylated TBK1 was predominantly detected in Parkin puncta in R-TBK1 expressing cells, although the clear accumulation of R-TBK1 in Parkin puncta was not observed (Supplementary Material, Fig. S5B). In contrast, the R-TBK1-K38M mutant significantly prevented p62 S403 phosphorylation and degradation during CCCP treatment (Fig. 4E). These results suggest that the local concentration of TBK1 at Parkin puncta determines its activity.

Optineurin recruits TBK1 to depolarized mitochondria

How is TBK1 specifically recruited to the Parkin-recruited mitochondria? As OPTN has been proposed as an important factor for the optimal activation and function of TBK1 (32,33) and recently reported as an autophagy receptor for damaged mitochondria in Parkin-mediated mitophagy (34), OPTN may participate in the TBK1 relocation and activation during Parkin-dependent mitophagy. To evaluate this possibility, we generated a G-Parkin and R-OPTN double-stable N2a cell line and monitored the R-OPTN relocation to Parkin puncta during CCCP treatment. After a 3-h CCCP treatment, several but not all Parkin puncta were co-localized with R-OPTN. The OPTN-positive Parkin puncta contained S172-phospho-TBK1 and S403-phospho-p62 (Fig. 5A and B). We also confirmed that the endogenous OPTN was co-localized with Parkin puncta that contained S403-phospho-p62 (Supplementary Material, Fig. S5). Active TBK1 was observed

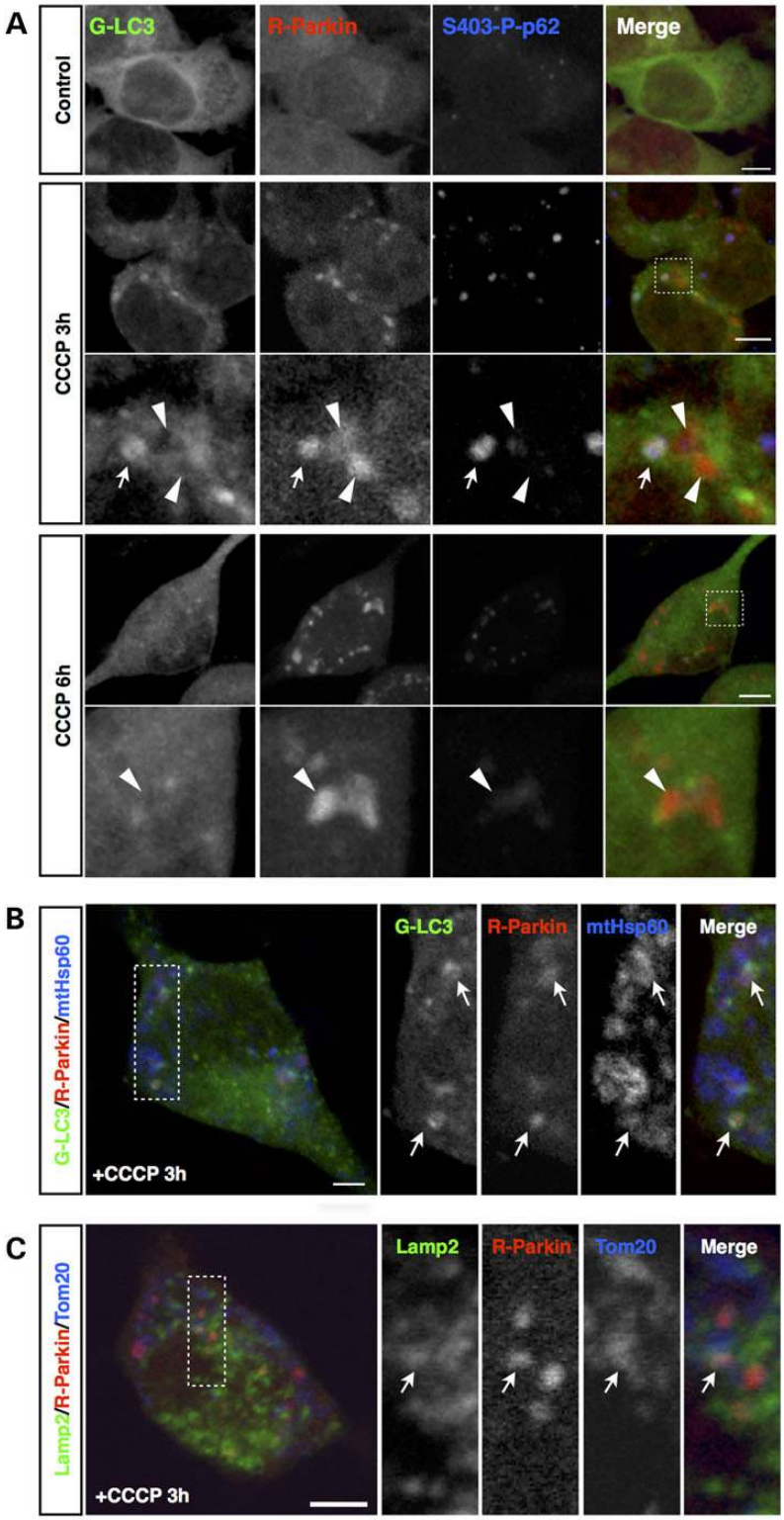

Figure 2. Autophagosome selectively engulfs phospho-p62-positive mitochondria. (**A**) G-LC3 and R-Parkin double-stable N2a cells were treated with 25 μM CCCP for indicated periods, and G-LC3 (green), R-Parkin (red) and S403-phospho-p62 (S403-P-p62, blue) were visualized by confocal microscopy. Magnified images representing the square region in merged images are shown. Arrows and arrowheads indicate autophagosome surrounding Parkin puncta with and without G-LC3, respectively. Scale bar = 5 μm. (**B**) Cells in A were treated with 25 μM CCCP for 3 h, and G-LC3 (green), R-Parkin (red) and mitochondrial Hsp60 (mtHsp60, blue) were visualized by confocal microscopy as indicated. Magnified images representing the rectangle region were generated in each fluorophore as indicated. Arrows indicate Parkin puncta co-localizing with both G-LC3 (autophagosome) and mtHsp60 (mitochondria). Scale bar = 5 μm. (**C**) N2a R-Parkin cells were treated with 25 μM CCCP for 3 h, and Lamp2 (green), R-Parkin (red) and Tom20 (blue) were visualized by confocal microscopy as indicated. Magnified images representing the rectangle region were generated in each fluorophore as indicated. Arrows indicate Parkin-recruited mitochondria co-localizing with Lamp2 (lysosome). Scale bar = 5 μm.

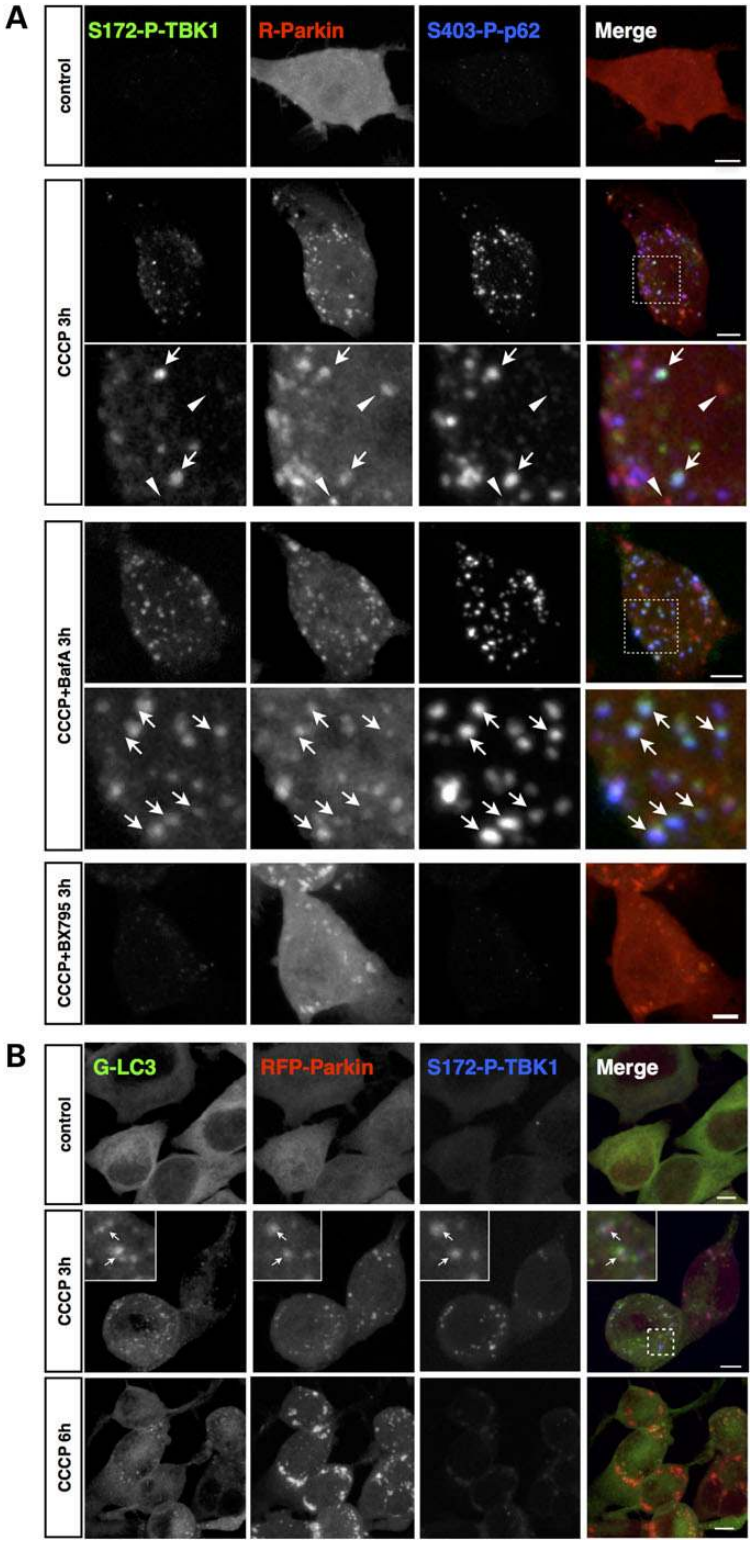

Figure 3. TBK1 is activated in Parkin puncta, and the activated TBK1 is co-localized with S403-phospho-p62. (**A**) N2a R-Parkin cells were treated with or without 25 μM CCCP, 1 μM BafA and 1 μM BX795 for 3 h as indicated. S172-phospho-TBK1 (S172-P-TBK1, green), R-Parkin (red) and S403-phospho-p62 (S403-P-p62, blue) were visualized by confocal microscopy. Magnified image representing the square region in merged images was shown. Arrows and arrowheads indicate Parkin puncta with both S172-phospho-TBK1 and S403-phospho-p62 and Parkin puncta without phospho-TBK and phospho-p62, respectively. Scale bar = 5 μm. (**B**) G-LC3 and R-Parkin double-stable N2a cells were treated with 25 μM CCCP for indicated periods, and G-LC3 (green), R-Parkin (red) and S172-phospho-TBK1 (S172-P-TBK, blue) were visualized by confocal microscopy. Insets are the magnified image representing the square region in merged images. Arrows indicate S172-phospho-TBK1-positive Parkin punctum surrounded by G-LC3. Scale bar = 5 μm.

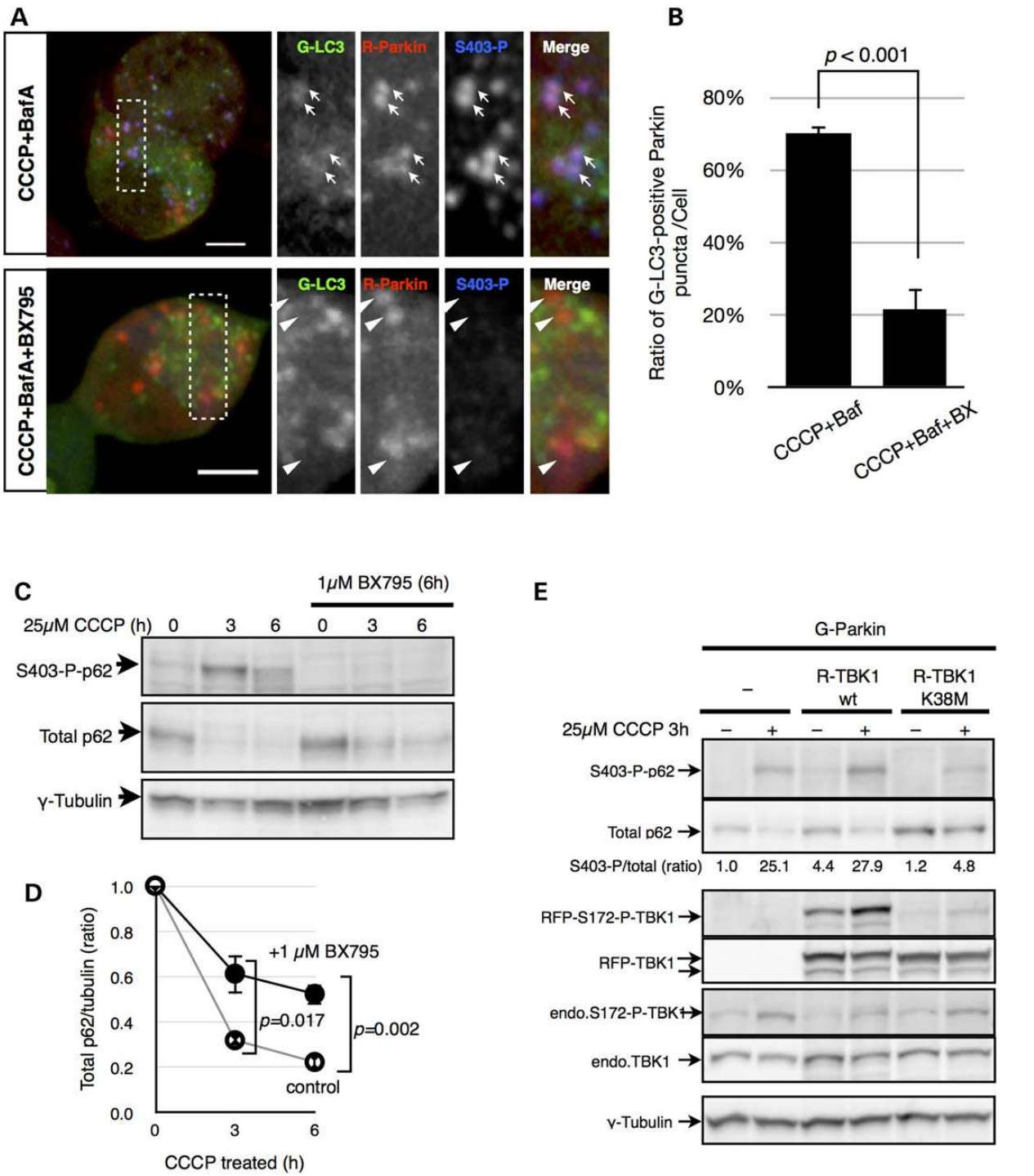

Figure 4. TBK1 inhibition prevents p62-mediated autophagosomal engulfment of Parkin-recruited mitochondria. (**A**) G-LC3 and R-Parkin double-stable N2a cells were treated with 25 μM CCCP, 1 μM BafA and 1 μM BX795 for 3 h as indicated. G-LC3 (green), R-Parkin (red) and S403-phospho-p62 (S403-P, blue) were visualized by confocal microscopy. Magnified images corresponding to rectangle region were generated in each fluorescence channel as indicated. Arrows and arrowheads indicate Parkin puncta co-localized with and without both G-LC3 and S403-phospho-p62, respectively. Scale bar = 5 μm. (**B**) Numbers of Parkin puncta co-localized with or without G-LC3 in a cell were counted, and the averaged ratio of G-LC3-positive Parkin puncta out of total Parkin puncta in nine different cells is shown. Error bar represents SEM ($n = 9$) and *P*-value of Student's *t*-test. (**C**) N2a R-Parkin cells were treated with 25 μM CCCP for the indicated periods, simultaneous treatment of BX795 or not for 6 h as indicated. The amount of S403-phospho-p62, total p62 and γ-tubulin were analyzed by western blotting. (**D**) The relative amount of p62 normalized with γ-tubulin were measured and plotted against the CCCP treatment time (hour). Closed circle indicates BX795-treated cell, and open circle represents control. Error bar represents SEM ($n = 4$), and *P*-value (Student's *t*-test) is shown. (**E**) N2a G-Parkin cells stably expressing R-TBK1 wild type or K38M mutant were treated with or without 25 μM CCCP for 3 h as indicated. Cell lysates were subjected to immunoblotting analysis using indicated antibodies.

only in Parkin puncta, even though many OPTN puncta without Parkin existed throughout the cell. Only a limited fraction of endogenous or overexpressed TBK1 is recruited to Parkin puncta (Supplementary Material, Fig. S5A). As active TBK1 and OPTN are absent in mitochondria clusters (Figs 2, 3B bottom and 5C), TBK1 recruitment and activation by OPTN at Parkin-recruited mitochondria may be a critical step for the p62-mediated mitophagy.

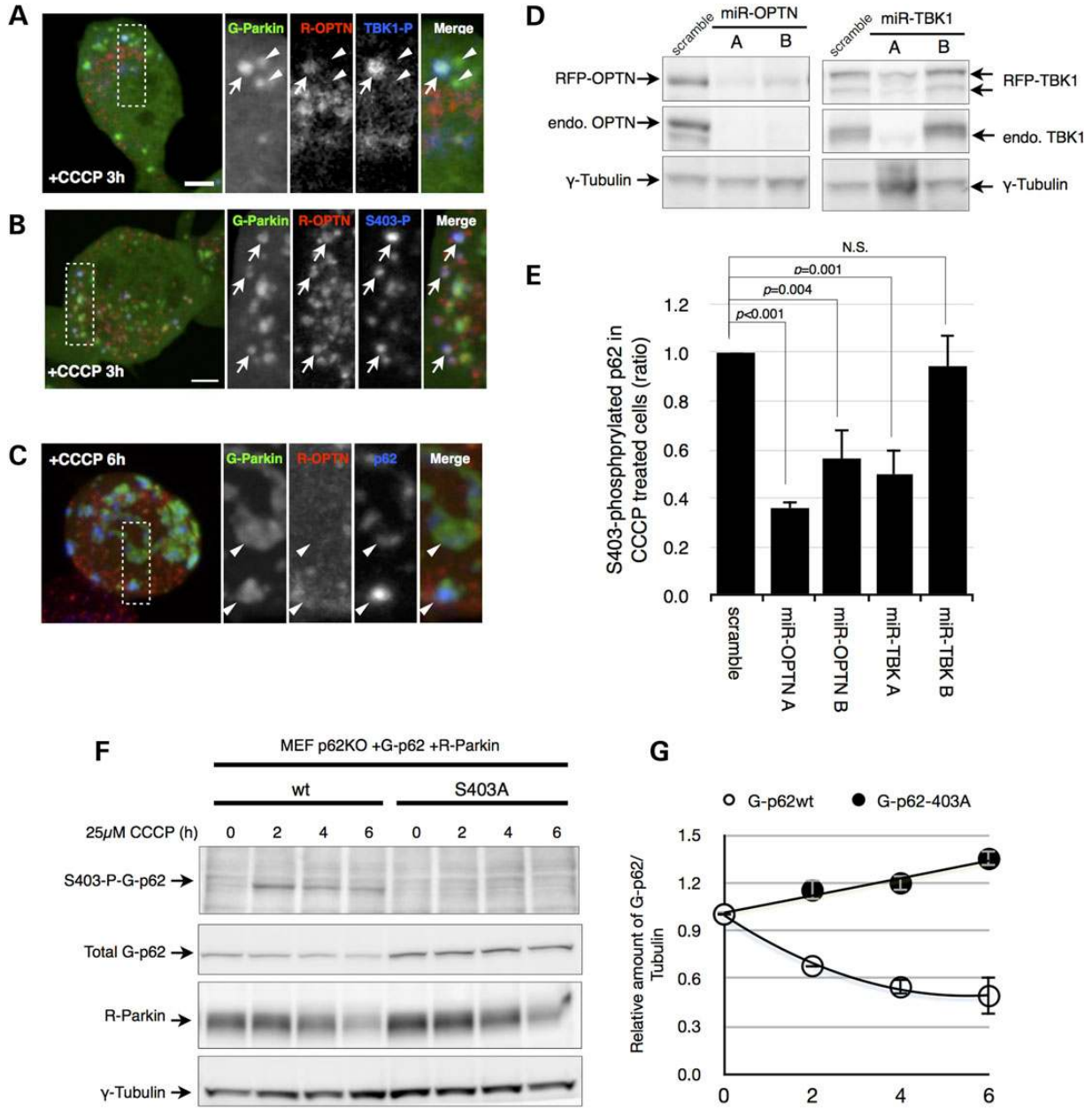

Figure 5. OPTN recruits TBK1 to depolarized mitochondria for its activation. (**A**) G-Parkin and R-OPTN double-stable N2a cells were treated with or without 25 μM CCCP for 3 h. G-Parkin (green), R-OPTN (red) and S172-phospho-TBK1 (S172-P-TBK, blue) were visualized by confocal microscopy. Magnified images corresponding to the rectangle region in merged image were generated in each fluorophore as indicated. Arrows and arrowheads indicate Parkin puncta containing both R-OPTN and S172-phospho-TBK1 and Parkin puncta without R-OPTN, respectively. Scale bar = 5 μm. (**B**) G-Parkin (green), R-OPTN (red) and S403-phospho-p62 (S403-P-p62, blue) in cells described in A were visualized by confocal microscopy, and magnified images representing the rectangle region were shown in each fluorophore as indicated. Arrows indicate Parkin puncta containing both OPTN and S403-phospho-p62. Scale bar = 5 μm. (**C**) Cells in A and B were treated with 25 μM CCCP for 6 h. G-Parkin (green), R-OPTN (red) and endogenous total p62 (p62, blue) were visualized by confocal microscopy. Magnified images corresponding to the rectangle region were generated in each fluorophore as indicated. Arrowheads indicate mitochondria cluster. Scale bar = 5 μm. (**D**) Confirmation of RNAi efficiency. miR-RNAi plasmids, RFP-TBK1 and RFP-OPTN plasmids were transiently co-transfected into N2a G-Parkin cells as indicated. After 48 h of transfection, cells were subjected to immunoblotting analysis. Overexpressed and endogenous amounts of OPTN and TBK1 are shown. (**E**) N2a G-Parkin cells were transiently transfected with an RFP and miR-RNAi expressing vector as indicated. After 48 h of transfection, cells were treated with 25 μM CCCP for 3 h, and the amounts of S403-phosphorylated p62 normalized with γ-tubulin are shown. Error bar represents SEM ($n = 3$), and *P*-value (Student's *t*-test) is shown. (**F**) p62 knockout MEF with G-p62 wild-type or S403A-mutant cells were transiently transfected with R-Parkin as indicated. After 48 h of transfection, cells were treated with 25 μM CCCP for indicated periods and subjected to immunoblotting analysis. S403-phosphorylated or total amount of G-p62 and γ-tubulin are shown. (**G**) The relative amount of G-p62 wild type (open circle) and S403A mutant (closed circle) normalized with γ-tubulin is shown. Error bar represents SEM ($n = 3$).

To investigate whether OPTN and TBK1 are required for the p62-mediated mitophagy, we performed RNA interference (RNAi) experiments (Fig. 5D and E). The expression of microRNA-derived RNAi (miR) against OPTN and TBK1 remarkably repressed S403 phosphorylation of p62 according to the knockdown efficiency, although the miR-TBK1 B construct failed to knockdown TBK1 expression. These results suggest that TBK1 activation and p62 S403 phosphorylation occur after TBK1 recruitment and OPTN and TBK1 are crucial for inducing p62-mediated mitophagy.

p62 phosphorylation is required for p62-mediated mitophagy

Because TBK1 phosphorylates OPTN at S177 and the phosphorylation enhances OPTN–LC3 interaction followed by subsequent autophagic degradation in xenophagy (35), it may be possible that S177 phosphorylation of OPTN by TBK1 is sufficient to promote mitophagy without p62. To evaluate this possibility, we developed wild-type or S403A-mutant G-p62 stably expressing p62 knockout mouse embryonic fibroblast (MEF) cells, and R-Parkin was transiently transfected in these cells. If p62 phosphorylation could be a byproduct in mitophagy, S403A-mutant p62 should be efficiently degraded during CCCP treatment as well as wild type. Wild-type G-p62 in p62 knockout MEF cells was transiently phosphorylated at S403 and efficiently degraded by CCCP treatment, whereas G-p62-S403A mutant was resistant to mitophagy-induced degradation, suggesting that S403 phosphorylation is essential for its degradation during mitophagy (Fig. 5F and G). To assess the contribution of p62 in mitophagy, we measured the ratio of Parkin puncta with LC3 in the R-Parkin-transfected p62 knockout MEF cells (Fig. 6). As expected, Parkin puncta was appeared by 2 h of treatment with CCCP, and OPTN and TBK1 were also found in Parkin puncta, suggesting that their recruitment to Parkin puncta was independent of p62 (Fig. 6A). By the treatment, ~38% of Parkin puncta were co-localized with LC3, whereas the co-expression of p62 enhanced the autophagosomal engulfment of Parkin puncta up to 58% (Fig. 6B–D). These results suggest that p62 has an important role in the clearance of damaged mitochondria, although the absence of p62 can be partially compensated.

Discussion

In this study, we demonstrate that TBK1 controls p62-mediated autophagosomal engulfment through S403 phosphorylation of p62. Because S403 phosphorylation enhances p62–polyubiquitin interaction (6), it has been believed that S403 phosphorylation is required for targeting of ubiquitinated substrates. However, our current results reveal that the S403-phosphorylated p62 is required for its efficient autophagosomal engulfment and can be a marker for the true autophagic cargo. Intriguingly, other autophagic adapter protein, OPTN, regulates this phosphorylation process through TBK1 activation. These factors are also known as xenophagy regulators (11,35). Recently, the functional link between mitophagy and xenophagy was predicted (36), and our results also support the idea that the selective autophagy processes after cargo polyubiquitination may be conserved between mitophagy and xenophagy. Since the evolutionary origin of the mitochondrion is a bacterial endosymbiont, cells may recognize dysfunctional mitochondria as harmful bacterial pathogens that produce cytotoxic ROS.

We propose the following molecular mechanism of p62-mediated autophagic engulfment of Parkin-recruited damaged mitochondria (Fig. 7). A depolarized mitochondria is recognized by PINK1-Parkin system and conjugated with K63-linked polyubiquitin chains by Parkin (19,36,37). p62 recognizes polyubiquitinated substrates as unwanted waste. Since OPTN and TBK1 form a stable complex in cells (32) and OPTN binds polyubiquitin chain (38–41), the OPTN–TBK1 complex is simultaneously recruited to the ubiquitin-coated waste. Other TBK1 binding adaptor proteins, such as TANK, NAP1, SINTBAD and NDP52 (40,42), may be potentially possible to contribute to TBK1 recruitment as well as OPTN. TBK1 activation is primarily controlled by its local concentration through a trans-autophosphorylation mechanism (28,29,43). Thus, the locally concentrated TBK1 at ubiquitin-coated waste can be activated by trans-autophosphorylation. The activated TBK1 phosphorylates p62 at S403, and the ubiquitin-coated waste becomes an 'autophagic cargo' that is subsequently engulfed by autophagosomes. Because the S403 phosphorylation of p62 stabilizes the interaction between p62 and the polyubiquitin chain (6), the S403-phospho-p62 efficiently anchors an LC3-positive phagophore (also called an isolation membrane) at the autophagic cargo and may facilitate autophagosome development. Phagophores attached to non-phospho-p62, meanwhile, are easily released from the cargo because of a weak interaction. This idea is supported by our previous observation that S403E-mutant p62, which mimics S403-phosphorylated p62, forms stable p62 bodies with ubiquitinated protein, whereas S403A-mutant p62 bodies are highly dynamic (6). Thus, we propose that p62 phosphorylation at S403 is an appropriate marker for the autophagic cargo that is subsequently engulfed by autophagosomes, whereas the ubiquitin-coated waste accumulates with non-phosphorylated p62 when OPTN–TBK1 recruitment fails.

It is controversial whether p62 is required for mitophagy (26,37,44,45). The controversy of the p62 requirement is based on the assumption that p62-mediated mitophagy continues all through the CCCP-treated period and mitophagy is assayed by counting cells that lost mitochondrial signals after mitochondria cluster formation. Our results show that p62-mediated mitophagy contributes the efficient targeting of Parkin-recruited mitochondria to autophagosomes, in which the S403 phosphorylation by TBK1 is required (Figs 4 and 6), whereas S403-phospho-p62-dependent selective autophagy is terminated after mitochondria cluster formation (Fig. 1B, Supplementary Material, Figs S1C and 2A). These findings may indicate that the p62-mediated mitophagy occurs only in the acute phase of mitochondrial depolarization. On the other hand, the significant numbers of Parkin puncta were engulfed by autophagosome without p62 in p62 knockout MEF cells (Fig. 6). This may be explained as the other autophagy adaptors, for example, NBR1, Nix or Fundc1, could compensate p62 functions or the conventional non-selective macroautophagy also participates in the engulfment of Parkin-recruited mitochondria by autophagosomes. As depolarization of all mitochondria never occurs under the physiological conditions, the p62-mediated mitophagy system would be enough to conduct the immediate clearance of damaged mitochondria.

The previous research (34,35) and our current results reveal that OPTN has critical functions in both xenophagy and mitophagy as well as p62. As OPTN and p62 bind to a different sub-domain in bacteria (35) and have distinct kinds of ubiquitin-binding motifs, such as ubiquitin-binding ABIN and NEMO (UBAN) and UBA domains, respectively (41), they recognize different targets at the autophagic cargo. Most of the p62 co-localizes in the mitochondrial clusters upon CCCP treatment (Fig. 1A and Supplementary Material, Fig. S1A), but OPTN was not detected in them (Supplementary Material, Fig. S5B), indicating that OPTN may not bind to the K63-linked polyubiquitin chain that is conjugated by Parkin. What does OPTN bind to in the Parkin-recruited

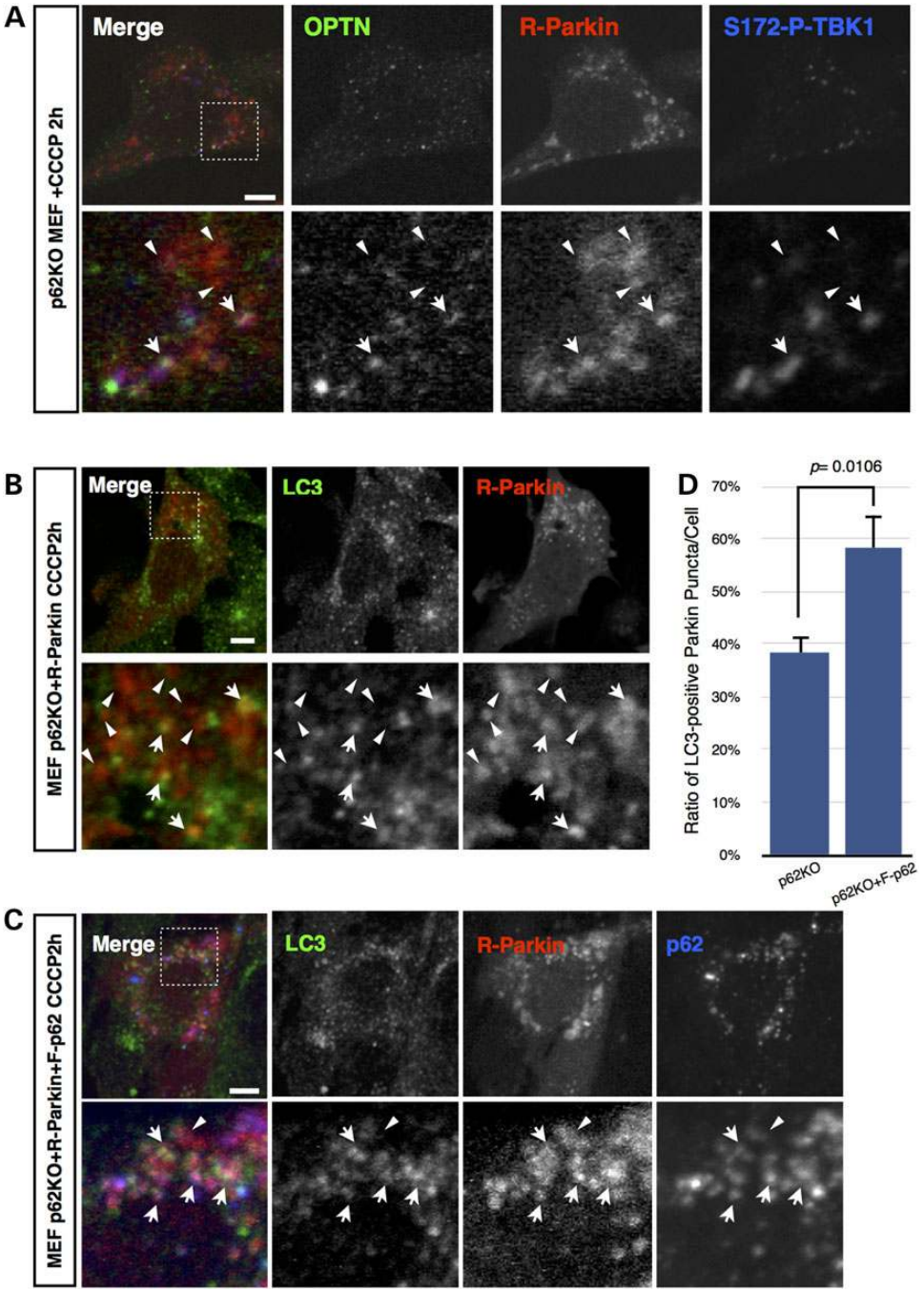

Figure 6. p62 is required for the efficient mitophagy. (**A**) p62 knockout MEF cells were transfected with R-Parkin, and cells were treated with 25 μM CCCP for 2 h. Endogenous OPTN (green), R-Parkin (red), and S172-phospho-TBK1 (S172-P-TBK; blue) were visualized by confocal microscopy. Magnified images corresponding to the square region in merged image were generated in each fluorophore as indicated. Arrows and arrowheads indicate Parkin puncta containing both OPTN and S172-phospho-TBK1 and Parkin puncta without OPTN and S172-phospho-TBK1, respectively. Scale bar = 5 μm. (**B** and **C**) p62 knockout MEF cells were transfected with R-Parkin (B) or R-Parkin together with FLAG-tagged wild-type human p62 (C). After 24 h of transfection, cells were treated with 25 μM CCCP for 2 h. Endogenous LC3 (green), R-Parkin (red) and transfected FLAG-p62 (blue) were visualized by confocal microscopy as indicated. Arrows and arrowheads indicate Parkin puncta co-localized with LC3 and Parkin puncta without LC3, respectively. Scale bar = 5 μm. (**D**) The total numbers of Parkin punctum and Parkin puncta containing LC3 were counted, and a ratio between the number of Parkin punctum co-localized with LC3 and total Parkin puncta in each cells was determined. More than 200 individual Parkin puncta in each condition were analyzed. Error bar represents SEM ($n = 5$), and *P*-value (Student's *t*-test) is shown.

mitochondria? As OPTN is absent in intact (healthy) mitochondria and mitochondrial clusters, the target molecule for OPTN binding may only transiently exist in the Parkin-recruited mitochondria. Moreover, since OPTN knockdown represses TBK1-mediated p62 phosphorylation upon CCCP treatment, a mechanism for the recruitment of the OPTN–TBK1 complex may distinguish autophagic cargo that has to be eliminated immediately. Further analysis is needed to clarify how the OPTN–TBK1 complex is recruited to selected autophagic cargo for the efficient clearance of cellular wastes.

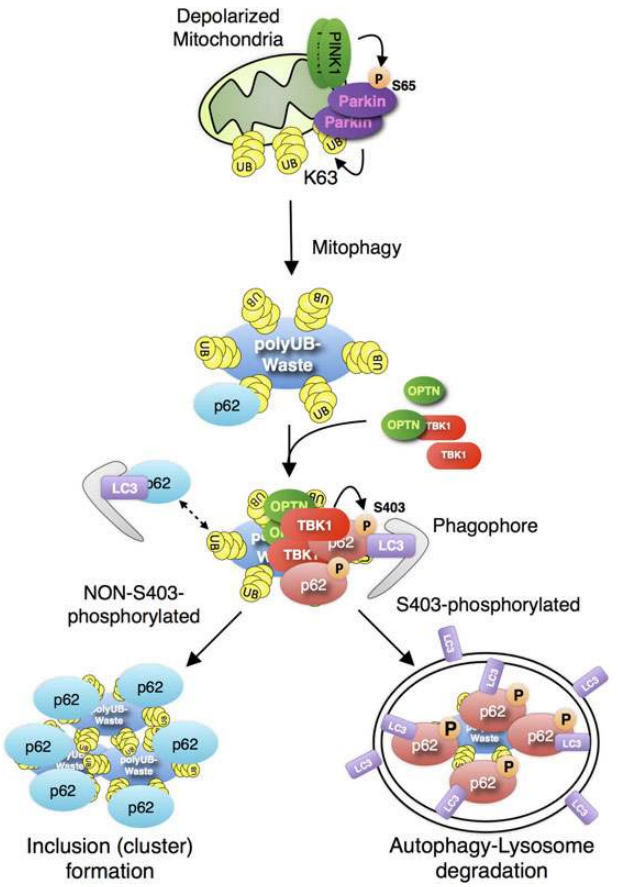

Figure 7. A model for p62-mediated selective autophagy. Schematic representation of the proposed molecular mechanism for p62-mediated selective autophagy. Depolarized mitochondria are marked with a polyubiquitin chain that is conjugated by specific ubiquitin E3 ligases including Parkin. Unphosphorylated p62 proteins, which exist abundantly in cytoplasm, weakly bind to the K63-linked polyubiquitin-conjugated unwanted waste. OPTN (or other TBK1 binding adaptor proteins) recruits TBK1 to the ubiquitin-coated waste, and then TBK1 gets activated through trans-autophosphorylation. The active TBK1 phosphorylates p62 at S403, and the S403-phosphorylated p62, which is a high ubiquitin-binding form, can tether phagophores to the autophagic cargo, allowing efficient autophagosome development. The TBK1-absent cargoes allow phagophore release, resulting in the failure of autophagosomal engulfment. When the autophagic cargo production exceeds the capacity of selective autophagy, the cargoes fuse to each other and may form a cytoplasmic inclusion body.

Materials and Methods

Cell culture and plasmids

All cells were maintained at 37°C in a 5% CO_2-humidified atmosphere in Dulbecco's modified Eagle's medium supplemented with 10% fetal bovine serum (FBS), 100 U/ml penicillin, 100 μg/ml streptomycin and/or 200 μg/ml Kanamycin (Wako). N2a-derived stable cell lines were maintained with further addition of 200 μg/ml hygromycin (Wako) and/or 400 μg/ml G418 (InvivoGen).

Stable cell lines were derived from the Flp-in Neuro2a (N2a/FRT) cell line described previously (6). R-Parkin and G-Parkin lines were generated by transfection with pmRFP-Parkin or pEGFP-Parkin, respectively, into N2a/FRT followed by drug selection with 400 μg/ml G418. G-LC3+R-Parkin wild-type (JTI-G-LC3+R-Parkin-wt) or K161-mutant (JTI-G-LC3+R-Parkin-K161N) lines were generated by transfection with pmRFP-Parkin (wild type) or pmRFP-Parkin-K161N, respectively, in the N2a JTI-LC3 line, which is generated by transfection with pJTI-G-LC3 in the N2a/FRT line followed by drug selection with 300 g/ml hygromycin, and were selected by 400 μg/ml G418 resistance. N2a JTI-G-Parkin+R-OPTN and N2a JTI-G-Parkin+R-TBK1 cell lines were generated by transfections with pmRFP-OPTN and peRFP-TBK1, respectively, in the N2a JTI-G-Parkin cell line, which is generated using Jump-In™ Cell Engineering Platform system (Life Technologies) by transfection with both pJTI-GFP-Parkin and pJTI-PhiC31-Int (Life Technologies) in the N2a/FRT cell line followed by 300 μM hygromycin. N2a R-Parkin G-p62 wild-type cell line was generated using Flp-In™ Cell Line Development system (Life Technologies) by transfection with pOG44 (Life Technologies) and pFRT-G-p62wt in the N2a R-Parkin parent cell line, which is a derivative of the N2a/FRT cell line. Drug-resistant cells were sub-cloned into more than ~90% homogeneity. Gene transfections were performed using LipofectAmine2000 reagent (Life Technologies) according to the manufacturer-recommended amount. The expression of each protein in generated cell lines was verified by western blotting using appropriate antibodies. p62 knockout MEF cells were generated from p62 knockout mouse (kindly gifted from Dr Tetsuro Ishii, Tsukuba University) and immortalized with SV40T antigen (kindly gifted from Dr Yusuke Yanagi, Kyushu University). pJTI-G-p62 wild type or pJTI-G-p62-S403A and pJTI-PhiC31-Int were transfected into the sub-cloned immortalized p62 knockout MEF cells by LipofectAmine 2000 reagent, and hygromycin-resistant stable cell lines were developed using Jump-In™ Cell Engineering Platform system (Life Technologies).

For plasmid construction, we used the Gateway® system (Life Technologies). The human Parkin gene was amplified from pcDNA-FLAG-Parkin (kindly gifted by Dr Ryosuke Takahashi, Kyoto University), and mouse TBK1 and OPTN genes were amplified from a mouse cDNA library with an attL sequence, using the following primer sets (Life Technologies); attL (attL1-F: 5′ GGGCCCCAAATAATGATTTTATTTTGACTGATAGTGACCTGTTCGT TGCAACAAATTGATGAGCAATGCTTTTTTTATAATGCCAACTTTGTA CAAAAAAG 3′, att2-R: 5′ GGATGGCAAATAATGATTTTATTTTGACT GATAGTGACCTGTTCGTTGCAACAAATTGATAAGCAATGCTTTCTT ATAATGCCAACTTTGTACAAGAAAGC 3′), gw-Parkin (F: 5′ GAATTC TTTTAGATCTACCATGATGATAGTGTTTGTCAGGTTCAAC 3′, R: 5′ GTAAAATCTAGATCACACGTCAAACCAGTGATCTCCCATGC 3′), gwL-TBK1 (F: 5′ ATGCCAACTTTGTACAAAAAAGCAGGCTCGAC CATGCAGAGCACCTCCAACCATCTGTGGCTCCTG 3′, R: 5′ CTTA TAATGCCAACTTTGTACAAGAAAGCTGGGTTCAAAGACAGTCCAC ATTGCGAAGGCCACCATC 3′) and gwL-OPTN (F: 5′ CGAATTCTTT TAGATCTACCATGTCCCATCAACCTCTGAGCTGCCTGACTG 3′, R: 5′ AAAGCTGGGTAAAATCTAGATCAAATGATGCAGTCCATCACAT GGATCTG 3′). The amplified fragments were cloned into pmRFP-N1-DEST (6) using Gateway® system or pEGFP-N1-DEST, in which NheI and HindIII fragment of EGFP from pEGFP-C1 (TAKARA BIO) was inserted into the same sites of pmRFP-N1-DEST. Mutations in Parkin or TBK1 were introduced by QuickChange site-directed mutagenesis methods using PrimeSTAR® Max DNA polymerase (TAKARA BIO) and following primer and their reverse complementary primer sets: Parkin-K161N (5′ GGC CCCTGTCAAAGAGTGCAGCCGGGAAATCTCAGGGTACAGTGCAGC ACCTGCAGGCAG 3′), D280N (5′ GACAAGACTCAATGATCGGCA GTTTGTTCACAACCCTCAACTTGGCTACTCCCTGCCTTGTGTG 3′), G430D (5′ CGCTGCCATGTACCAGTGGAAAAAAATGGAGACTGCAT GCACATGAAGTGTCCGCAGCCCCAG 3′) and TBK1-K38M (5′ CATA AGAAAACTGGTGATCTCTATGCTGTCATGGTATTTAATAACATAAG CTTCCTTCGCCCAG 3′).

To generate microRNA expression vectors for RNAi experiments, double-stranded oligo DNA for miR-OPTN (A: 5′ TGCTG TTGAGCTGCAGTTCTGAGACGGTTTTGGCCACTGACTGACCGTCTC AGCTGCAGCTCAA 3′ and 5′ CCTGTTGAGCTGCAGCTGAGACGGTC AGTCAGTGGCCAAAACCGTCTCAGAACTGCAGCTCAAC 3′, B: 5′ TG CTGATCAGGGACTGTCTACTGCCTGTTTTGGCCACTGACTGACAGG CAGTACAGTCCCTGAT 3′ and 5′ CCTGATCAGGGACTGTACTGCC TGTCAGTCAGTGGCCAAAACAGGCAGTAGACAGTCCCTGATC 3′) or miR-TBK1 (A: 5′ TGCTGTTCTGATGGTCCTTTCTTAGCGTTTT GGCCACTGACTGACGCTAAGAAGACCATCAGAA 3′ and 5′ CCTGT TCTGATGGTCTTCTTAGCGTCAGTCAGTGGCCAAAACGCTAAGAAA GGACCATCAGAAC 3′, B: 5′ TGCTGAGAACTGGAAAGTCTCAGCAGG TTTTGGCCACTGACTGACCTGCTGAGTTTCCAGTTCT 3′ and 5′ CCT GAGAACTGGAAACTCAGCAGGTCAGTCAGTGGCCAAAACCTGCT GAGACTTTCCAGTTCTC 3′) was inserted into precut sites of the pcDNA6.1-RFP-miR vector as described previously (6).

Antibodies

Anti-phospho-p62 (S403) clone 4F6 antibodies were described previously (6) and are now available from MBL (D343-3) and Millipore (MABC186). Anti-p62 (monoclonal 5F2, MBL; polyclonal PM045, MBL and polyclonal C-terminal p62 PM066, MBL), anti-RFP (polyclonal PM005, MBL), anti-multiubiquitin (FK2, MBL), anti-TBK/NAK (EPR2867(2)-19; abcam), anti-S172-phospho-TBK (D52C2; Cell signaling for immunocytochemistry), anti-NAK (phospho S172) (EPR2867(2), abcam for western blotting), anti-Tom20 (sc-11415, Santa Cruz), anti-Hsp60 (sc-1052, Santa Cruz), anti-OPTN (sc-166576, C-2, Santa Cruz), anti-LC3 (D3U4C, Cell Signaling Technology), anti-Lamp-2 (ABL-93, Southern Biotech) and anti-γ-tubulin (GTU-88, Sigma) were purchased from the indicated vendors.

Immunofluorescence microscopy

For co-localization studies, cells were grown in Matrigel-coated (Corning), four-well glass slide chambers (Lab-Tek). Drug-treated N2a-derived cell lines were fixed in 4% formaldehyde in phosphate-buffered saline (PBS) for 10 min, blocked with 2% FBS and 1% Triton X-100 in PBS with 200 mM imidazole and 100 mM NaF. Fixed cells were incubated with appropriate primary antibodies in the blocking buffer, then with AlexaFluor 488- or 633-conjugated anti-rabbit, rat, goat or mouse IgG (Life Technologies) after washing with PBS+0.1% Triton X-100 and mounted in VECTASHIELD® Mounting Medium (Vector Laboratories). Confocal microscopy was performed using an Olympus FV-1000 inverted confocal microscope equipped with a 60× oil lens with 4× zoom power. A whole-cell Z stack (each slice = 0.5 μm) was acquired, and a maximum projection was created to visualize all fluorophores existing in a cell. For the co-localization analysis, single confocal layer images were used for the generation of the magnified images to exclude signals in different confocal layers. Numbers of Parkin puncta with RFP fluorescence co-localized with or without GFP and/or Alexa488 fluorescence were counted manually (at least five different cells). All images were processed by Fluoview software (Olympus) or imageJ64 (NIH image).

Immunoblotting analysis

Cells were treated with or without 25 μM CCCP (Sigma), 1 μM BafA (SC Laboratories) and 1 μM BX795 (Calbiochem) as indicated and lysed with ultrasound in PBS with phosphatase inhibitors (2 mM imidazole, 1 mM NaF; Sigma) and protease inhibitor cocktail (Roche) or directly solubilized in sodium dodecyl sulfate (SDS) sample buffer. Boiled whole-cell lysates in SDS sample buffer were subjected to SDS–polyacrylamide gel electrophoresis (PAGE) followed by transfer to polyvinylidene difluoride membrane. After blocking with 3% goat serum (CEDERLANE) in PBS with 0.1% Triton X-100 (Sigma) and phosphatase inhibitors, the membrane was incubated with an appropriate primary antibody diluted in PBS+0.1% Triton X-100 containing 2% BSA and then with a secondary antibody conjugated with horseradish peroxidase (HRP) in PBS with 0.1% Triton X-100. Chemiluminescent signals by Western HRP substrate Luminata™ Forte (Millipore) were obtained and quantified using ImageQuant LAS-4000 (GE healthcare). Immunoblot analysis was repeated at least twice, and the results were confirmed more than three times with different sets of experiments.

Supplementary Material

Supplementary Material is available at *HMG* online.

Acknowledgements

We thank Ms Kiyoko Miyamoto for technical supports, Dr Ryosuke Takahashi (Kyoto University) for the kind gift of the human Parkin gene, Dr Tetsuro Ishii (Tsukuba University) for the kind gift of the p62 knockout mice for p62 knockout MEF cell development, Dr Yusuke Yanagi (Kyushu University) for the kind gift of the SV40T antigen plasmid, Dr Yuzuru Imai (Juntendo University) for helpful comments and the Support Unit for Bio-material Analysis, RIKEN BSI Research Resources Center and Research Support Center, Juntendo University Graduate school of Medicine for technical support.

Conflict of Interest statement. None declared.

Funding

This work was supported by Grants-in-Aid from the Ministry of Education, Culture, Sports, Science, and Technology (MEXT) of Japan to G.M. (23500434 and 24111554 for Scientific Research on Innovative Areas ‘Brain Environment’) and N.N. (22110004 for Scientific Research on Innovated Areas ‘Foundation of Synapse and Neurocircuit Pathology’, 22240037, 24659436 and 25253066), by Core Research for Evolutional Science and Technology (CREST) from Japan Science and Technology Agency to N.N., by a Grant-in-Aid for the Research on Measures for Ataxic Diseases from the Ministry of Health, Welfare and Labor to N.N. and by a Grant-in-Aid for Scientific Research on Innovative Areas ‘Brain Protein Aging and Dementia Control’ from MEXT to G.M. (15H01561) and N.N. (15H01567).

References

1. Mizushima, N. and Komatsu, M. (2011) Autophagy: renovation of cells and tissues. *Cell*, **147**, 728–741.
2. Rogov, V., Dötsch, V., Johansen, T. and Kirkin, V. (2014) Interactions between autophagy receptors and ubiquitin-like proteins form the molecular basis for selective autophagy. *Mol. Cell*, **53**, 167–178.
3. Birgisdottir, A.B., Lamark, T. and Johansen, T. (2013) The LIR motif—crucial for selective autophagy. *J. Cell Sci.*, **126**, 3237–3247.
4. Bjørkøy, G., Lamark, T., Brech, A., Outzen, H., Perander, M., Øvervatn, A., Stenmark, H. and Johansen, T. (2005) p62/SQSTM1 forms protein aggregates degraded by autophagy

and has a protective effect on huntingtin-induced cell death. *J. Cell Biol.*, **171**, 603–614.
5. Johansen, T. and Lamark, T. (2011) Selective autophagy mediated by autophagic adapter proteins. *Autophagy*, **7**, 279–296.
6. Matsumoto, G., Wada, K., Okuno, M., Kurosawa, M. and Nukina, N. (2011) Serine 403 phosphorylation of p62/SQSTM1 regulates selective autophagic clearance of ubiquitinated proteins. *Mol. Cell*, **44**, 279–289.
7. Walinda, E., Morimoto, D., Sugase, K., Konuma, T., Tochio, H. and Shirakawa, M. (2014) Solution structure of the ubiquitin-associated (UBA) domain of human autophagy receptor NBR1 and its interaction with ubiquitin and polyubiquitin. *J. Biol. Chem.*, **289**, 13890–13902.
8. Long, J., Gallagher, T.R.A., Cavey, J.R., Sheppard, P.W., Ralston, S.H., Layfield, R. and Searle, M.S. (2008) Ubiquitin recognition by the ubiquitin-associated domain of p62 involves a novel conformational switch. *J. Biol. Chem.*, **283**, 5427–5440.
9. Korolchuk, V.I., Mansilla, A., Menzies, F.M. and Rubinsztein, D.C. (2009) Autophagy inhibition compromises degradation of ubiquitin-proteasome pathway substrates. *Mol. Cell*, **33**, 517–527.
10. Kirkin, V., McEwan, D.G., Novak, I. and Dikic, I. (2009) A role for ubiquitin in selective autophagy. *Mol. Cell*, **34**, 259–269.
11. Pilli, M., Arko-Mensah, J., Ponpuak, M., Roberts, E., Master, S., Mandell, M.A., Dupont, N., Ornatowski, W., Jiang, S., Bradfute, S.B. *et al.* (2012) TBK-1 promotes autophagy-mediated antimicrobial defense by controlling autophagosome maturation. *Immunity*, **37**, 223–234.
12. Turowec, J.P., Duncan, J.S., French, A.C., Gyenis, L., St Denis, N. A., Vilk, G. and Litchfield, D.W. (2010) Protein kinase CK2 is a constitutively active enzyme that promotes cell survival: strategies to identify CK2 substrates and manipulate its activity in mammalian cells. *Meth. Enzymol.*, **484**, 471–493.
13. Zhao, W. (2013) Negative regulation of TBK1-mediated antiviral immunity. *FEBS Lett.*, **587**, 542–548.
14. Lin, M.T. and Beal, M.F. (2006) Mitochondrial dysfunction and oxidative stress in neurodegenerative diseases. *Nature*, **443**, 787–795.
15. Karbowski, M. and Neutzner, A. (2012) Neurodegeneration as a consequence of failed mitochondrial maintenance. *Acta. Neuropathol.*, **123**, 157–171.
16. Scherz-Shouval, R. and Elazar, Z. (2011) Regulation of autophagy by ROS: physiology and pathology. *Trends Biochem. Sci.*, **36**, 30–38.
17. Scarffe, L.A., Stevens, D.A., Dawson, V.L. and Dawson, T.M. (2014) Parkin and PINK1: much more than mitophagy. *Trends Neurosci.*, doi:10.1016/j.tins.2014.03.004.
18. Hattori, N., Saiki, S. and Imai, Y. (2014) Regulation by mitophagy. *Int. J. Biochem. Cell Biol.*, **53**, 147–150.
19. Lim, K.-L., Chew, K.C.M., Tan, J.M.M., Wang, C., Chung, K.K.K., Zhang, Y., Tanaka, Y., Smith, W., Engelender, S., Ross, C.A. *et al.* (2005) Parkin mediates nonclassical, proteasomal-independent ubiquitination of synphilin-1: implications for Lewy body formation. *J. Neurosci.*, **25**, 2002–2009.
20. Youle, R.J. and Narendra, D.P. (2011) Mechanisms of mitophagy. *Nat. Rev. Mol. Cell Biol.*, **12**, 9–14.
21. Sarraf, S.A., Raman, M., Guarani-Pereira, V., Sowa, M.E., Huttlin, E.L., Gygi, S.P. and Harper, J.W. (2013) Landscape of the PARKIN-dependent ubiquitylome in response to mitochondrial depolarization. *Nature*, **496**, 372–376.
22. Tanaka, A., Cleland, M.M., Xu, S., Narendra, D.P., Suen, D.-F., Karbowski, M. and Youle, R.J. (2010) Proteasome and p97 mediate mitophagy and degradation of mitofusins induced by Parkin. *J. Cell Biol.*, **191**, 1367–1380.
23. Yoshii, S.R., Kishi, C., Ishihara, N. and Mizushima, N. (2011) Parkin mediates proteasome-dependent protein degradation and rupture of the outer mitochondrial membrane. *J. Biol. Chem.*, **286**, 19630–19640.
24. Narendra, D., Tanaka, A., Suen, D.-F. and Youle, R.J. (2008) Parkin is recruited selectively to impaired mitochondria and promotes their autophagy. *J. Cell Biol.*, **183**, 795–803.
25. Matsuda, N., Sato, S., Shiba, K., Okatsu, K., Saisho, K., Gautier, C.A., Sou, Y.-S., Saiki, S., Kawajiri, S., Sato, F. *et al.* (2010) PINK1 stabilized by mitochondrial depolarization recruits Parkin to damaged mitochondria and activates latent Parkin for mitophagy. *J. Cell Biol.*, **189**, 211–221.
26. Geisler, S., Holmström, K.M., Skujat, D., Fiesel, F.C., Rothfuss, O.C., Kahle, P.J. and Springer, W. (2010) PINK1/Parkin-mediated mitophagy is dependent on VDAC1 and p62/SQSTM1. *Nat. Cell Biol.*, **12**, 119–131.
27. Kishore, N., Huynh, Q.K., Mathialagan, S., Hall, T., Rouw, S., Creely, D., Lange, G., Caroll, J., Reitz, B., Donnelly, A. *et al.* (2002) IKK-i and TBK-1 are enzymatically distinct from the homologous enzyme IKK-2: comparative analysis of recombinant human IKK-i, TBK-1, and IKK-2. *J. Biol. Chem.*, **277**, 13840–13847.
28. Ma, X., Helgason, E., Phung, Q.T., Quan, C.L., Iyer, R.S., Lee, M. W., Bowman, K.K., Starovasnik, M.A. and Dueber, E.C. (2012) Molecular basis of Tank-binding kinase 1 activation by transautophosphorylation. *Proc. Natl Acad. Sci. USA*, **109**, 9378–9383.
29. Larabi, A., Devos, J.M., Ng, S.-L., Nanao, M.H., Round, A., Maniatis, T. and Panne, D. (2013) Crystal structure and mechanism of activation of TANK-binding kinase 1. *Cell Rep.*, **3**, 734–746.
30. Tojima, Y., Fujimoto, A., Delhase, M., Chen, Y., Hatakeyama, S., Nakayama, K., Kaneko, Y., Nimura, Y., Motoyama, N., Ikeda, K. *et al.* (2000) NAK is an IkappaB kinase-activating kinase. *Nature*, **404**, 778–782.
31. Goncalves, A., Bürckstümmer, T., Dixit, E., Scheicher, R., Górna, M.W., Karayel, E., Sugar, C., Stukalov, A., Berg, T., Kralovics, R. *et al.* (2011) Functional dissection of the TBK1 molecular network. *PLoS ONE*, **6**, e23971.
32. Morton, S., Hesson, L., Peggie, M. and Cohen, P. (2008) Enhanced binding of TBK1 by an optineurin mutant that causes a familial form of primary open angle glaucoma. *FEBS Lett.*, **582**, 997–1002.
33. Gleason, C.E., Ordureau, A., Gourlay, R., Arthur, J.S.C. and Cohen, P. (2011) Polyubiquitin binding to Optineurin is required for optimal activation of TANK-binding kinase 1 and production of interferon β. *J. Biol. Chem.*, **286**, 35663–35674.
34. Wong, Y.C. and Holzbaur, E.L.F. (2014) Optineurin is an autophagy receptor for damaged mitochondria in Parkin-mediated mitophagy that is disrupted by an ALS-linked mutation. *Proc. Natl Acad. Sci. USA*, doi:10.1073/pnas.1405752111.
35. Wild, P., Farhan, H., McEwan, D.G., Wagner, S., Rogov, V.V., Brady, N.R., Richter, B., Korac, J., Waidmann, O., Choudhary, C. *et al.* (2011) Phosphorylation of the autophagy receptor optineurin restricts Salmonella growth. *Science*, **333**, 228–233.
36. Manzanillo, P.S., Ayres, J.S., Watson, R.O., Collins, A.C., Souza, G., Rae, C.S., Schneider, D.S., Nakamura, K., Shiloh, M.U. and Cox, J.S. (2013) The ubiquitin ligase Parkin mediates resistance to intracellular pathogens. *Nature*, **501**, 512–516.
37. Narendra, D., Kane, L.A., Hauser, D.N., Fearnley, I.M. and Youle, R.J. (2010) p62/SQSTM1 is required for Parkin-induced mitochondrial clustering but not mitophagy; VDAC1 is dispensable for both. *Autophagy*, **6**, 1090–1106.

38. Ryzhakov, G. and Randow, F. (2007) SINTBAD, a novel component of innate antiviral immunity, shares a TBK1-binding domain with NAP1 and TANK. *EMBO J.*, **26**, 3180–3190.
39. Korac, J., Schaeffer, V., Kovacevic, I., Clement, A.M., Jungblut, B., Behl, C., Terzic, J. and Dikic, I. (2012) Ubiquitin-independent function of Optineurin in autophagic clearance of protein aggregates. *J. Cell Sci.*, doi:10.1242/jcs.114926.
40. Chau, T.-L., Gioia, R., Gatot, J.-S., Patrascu, F., Carpentier, I., Chapelle, J.-P., O'Neill, L., Beyaert, R., Piette, J. and Chariot, A. (2008) Are the IKKs and IKK-related kinases TBK1 and IKK-epsilon similarly activated? *Trends Biochem. Sci.*, **33**, 171–180.
41. Kachaner, D., Génin, P., Laplantine, E. and Weil, R. (2012) Toward an integrative view of Optineurin functions. *Cell Cycle*, **11**, 2808–2818.
42. Thurston, T.L.M., Ryzhakov, G., Bloor, S., von Muhlinen, N. and Randow, F. (2009) The TBK1 adaptor and autophagy receptor NDP52 restricts the proliferation of ubiquitin-coated bacteria. *Nat. Immunol.*, **10**, 1215–1221.
43. Helgason, E., Phung, Q.T. and Dueber, E.C. (2013) Recent insights into the complexity of TANK-binding kinase 1 signaling networks: the emerging role of cellular localization in the activation and substrate specificity of TBK1. *FEBS Lett.*, **587**, 1230–1237.
44. Ding, W.-X., Ni, H.-M., Li, M., Liao, Y., Chen, X., Stolz, D.B., Dorn, G.W. and Yin, X.-M. (2010) Nix is critical to two distinct phases of mitophagy, reactive oxygen species-mediated autophagy induction and Parkin-ubiquitin-p62-mediated mitochondrial priming. *J. Biol. Chem.*, **285**, 27879–27890.
45. Okatsu, K., Saisho, K., Shimanuki, M., Nakada, K., Shitara, H., Sou, Y.-S., Kimura, M., Sato, S., Hattori, N., Komatsu, M. *et al.* (2010) p62/SQSTM1 cooperates with Parkin for perinuclear clustering of depolarized mitochondria. *Genes Cells*, **15**, 887–900.